Maintaining separation between airliners and RPAS in non-segregated airspace

M. Perez-Batlle, E. Pastor, X. Prats, P. Royo, and R. Cuadrado
ICARUS Research Group
Technical University of Catalonia
Esteve Terrades, 5. 08860 Castelldefels - Catalonia (Spain)

***Abstract*—When an airliner and a Remotely Piloted Air System (RPAS) have conflicting courses that may compromise the minimum safety separation between them, how much in advance should the RPAS start the separation manoeuvre? Which is the optimal heading change that will guarantee the desired separation distance with a minimum reaction time? These same questions can be asked if it is the airliner that performs the separation manoeuvre. In this paper the time reaction margins for both aircraft are analysed assuming they are equipped with Automatic Dependent Surveillance (ADS) systems able to exchange aircraft intents. Due to their small cruise speeds, RPAS manoeuvres must be initiated well before the airliner ones. This leads to some safety buffer in case the RPAS cannot comply with the required change of trajectory or if it becomes suddenly unresponsive (due to an internal failure or because a lost-link situation). The paper also assesses the operational point of view by simplifying the reaction times and conflict geometries by grouping them in a small set of cases, regarding the severity of a loss of separation event.**

***Keywords*—Separation conflicts; unmanned systems; airspace integration**

I. Introduction

The lack of consolidated regulations concerning remotely piloted air system (RPAS) certification, airworthiness and operations is still banning their civil use into non-segregated airspace. The pressure to integrate seamlessly their operations in civil aviation is increasing day by day and several institutions and safety agencies all around the globe are devoting significant efforts to this objective [1], [2], [3], [4]. Most of the remotely piloted aircraft (RPA) platforms that are likely to populate our skies in the future present flight performances (in terms of cruise speeds, bank angles, or climb/descent rates) significantly poorer than typical commercial airliners. However, they are expected to operate at very similar altitudes and therefore, separation and collision avoidance systems, mechanisms or procedures, well established nowadays in civil aviation, will have to be reviewed.

Extensive research has been devoted to collision avoidance algorithms that already take into account the particularities of RPAS. Most of the works inherit from robotics and control theory applications, like for instance [5], [6], [7], [8], [9], [10], [11]. Collision risk assessments for RPAS are also found in the literature [12], [13] which in turn, will set the basis to determine the required performances for the *sense and avoid* capabilities of the RPAS – one of the major challenges (at technological but also at regulatory levels[14]. Yet, few researchers have addressed the separation problem specifically for RPAS. Some proposals indeed, implement separation minima in their algorithms (like for example [6]), but they are in general, focused in very small RPA and typical separation values are in the order of meters. Yet, if bigger RPA are expected to fly into non-segregated airspace, larger separation values (such as 5 or 10 NM) will have to be considered[15].

SESAR and NextGen programs propose new paradigms that rely on accurate design and execution of four-dimensional trajectories that are expected to transition from radar control to trajectory-based operations. For example Airborne Separation Assurance Systems (ASAS) aim to delegate separation tasks from controllers to pilots or at least, enhance the situational awareness of the aircraft crew[16]. The accuracy of these systems, however, must rely on aircraft intent information. Otherwise, future flight paths can not be deduced with certainty from only past flight path information, current state vectors or by extrapolating (even with error free) the information of those state vectors[17]. Automatic Dependent Surveillance (ADS) systems, installed on-board the aircraft and transmitting its position and intentions, will likely be the enablers for future (self-)separation applications in manned or unmanned aviation.

In a first publication[18], the authors evaluated simple (but typical) conflict scenarios where heading changes were given to a RPAS in order to maintain a minimum separation distance with a much faster aircraft in a conflicting trajectory. As expected, results showed the importance of the relative speed between the two aircraft, being backward conflicts (the intruder chasing the RPA from behind) the most demanding ones. In [19], [20] a taxonomy for different conflict situations was proposed, along with possible separation assurance manoeuvres that could be undertaken by the RPAS.

In this paper it is supposed that both the RPAS and airliner are equipped with ADS systems and once the conflict is detected, the RPAS will initiate the separation manoeuvre. According to ADS standard radio frequency radiation patterns, we compute the earliest time a conflict can be detected for the RPAS and consequently, its reaction time window is derived.

Within this time window, the RPAS can initiate a heading change manoeuvre in such a way that the minimum separation is maintained between both aircraft. Then, an hypothetical case is considered where the RPAS does not actually execute the separation manoeuvre (considering, for instance, a loss-link emergency, a failure of the on-board separation assurance system or simply that is deemed more appropriate to solve the conflict by changing the airliner trajectory). Thus a new time window is computed showing the available margin for faster airliner to react.

The remaining of this paper is organised as follows. In Section II, the RPA-Airliner separation conflict is presented as a whole, in which any of both aircraft may perform the separation manoeuvre. It also describes the separation conflict model identifying the optimal separation heading changes. Section III explains in depth the proposed RPA separation manoeuvres. Section IV analyses the feasibility of the separation manoeuvres for the whole range of conflict geometries. Finally, Section V revisits the results obtained in the previous section adapting them to an operational perspective.

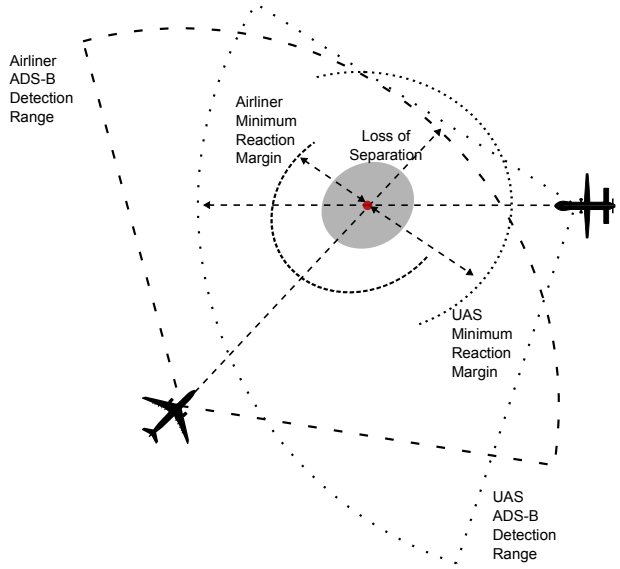

Fig. 1. Geometry of the conflict and reaction time windows for the UAS and the airliner.

II. RPA-Airliner Separation Conflicts as a Whole

Previous research by the authors has already investigated the way in which an RPA may execute a separation manoeuvre in case such a conflict exits with a much faster airliner [18], [19], [20]. However, the analysis so far has been performed under a simplified geometry and assuming that the RPA was always initiating the required separation reaction. Results showed some limitations in certain geometries. RPA typical slow speeds imply that higher separation angles are required to attain the same levels of separation compared to a typical conflict between two airliners. Moreover, RPA poor climb/descend performance also limit separation manoeuvres in the vertical plane. Speed adjustments show also some limitations and finally, but equally important, RPAs limited bank angles imply that the separation manoeuvre cannot be considered instantaneous and that the resulting separation turns need to be considered in the geometric models.

This section will revisit all the parameters indicated above under the light of our new objective; that is, understanding the RPA-airliner separation conflict as a whole, in which any of both vehicles may manoeuvre under the supervision of an air traffic control operator (ATCo). Additionally, the uncertainty produced by an unresponsive RPA needs also to be investigated, so that the full picture of the existing safety margins is understood. The final goal of the overall analysis is to prevent breaching the desired separation margins, thus avoiding that a mid-term separation conflict develops by action or inaction into a collision avoidance issue.

A. Separation Conflict Scenario

Figure 1 depicts the general scenario under analysis in this paper. Two aircraft, an airliner and a RPAS, have conflicting courses that may end up by loosing the desired horizontal separation distance between them (not necessarily ending up in a collision). At some point, the aircraft will identify the potential conflict, thanks to some on-board equipment such as ADS, a traffic information system (TIS) or simply because the ATCo will detect it. A first question could be: who should manoeuvre to avoid the separation conflict? Yet, it is out of the scope of this paper to assess this question, as it will depend on multiple factors such as: how is the traffic situation around both aircraft?, has the airliner somehow more *priority* over the RPA? etc.

Taking into account that the RPA will fly slower than the airliner, it will have to initiate the separation manoeuvre well in advance. In other words, once the conflict is detected, the RPA has less time to initiate the manoeuvre, should the minimum separation distance be respected. In this paper, we will compute these time windows or reaction margins, as shown in Figure 1, along with the optimal heading changes that guarantee the desired level of separation. Besides the conflict geometry, these margins strongly depend on the speed of both aircraft, but also on the bank angle capabilities of the manoeuvring aircraft.

Changing the altitude of one of the aircraft is indeed a possible solution to avoid the conflict. It should be noted, however, that this manoeuvre could not be effective if executed by the RPA, due to the extremely poor climbing (or even descending) performance that most of the RPA might have at typical mission altitudes (just few hundred feet per minute). Obviously, the airliner could always be the aircraft to change the flight level. Nevertheless, in this paper we focus only in lateral manoeuvres aiming at assessing their limits and safety time margins.

Figure 2 depicts the basics of the separation conflict scenario under consideration. A RPA and an airliner are both flying at a constant speed and altitude and they have conflicting straight trajectories (future work will need to consider the implications of any of both aircraft flying close to a turning

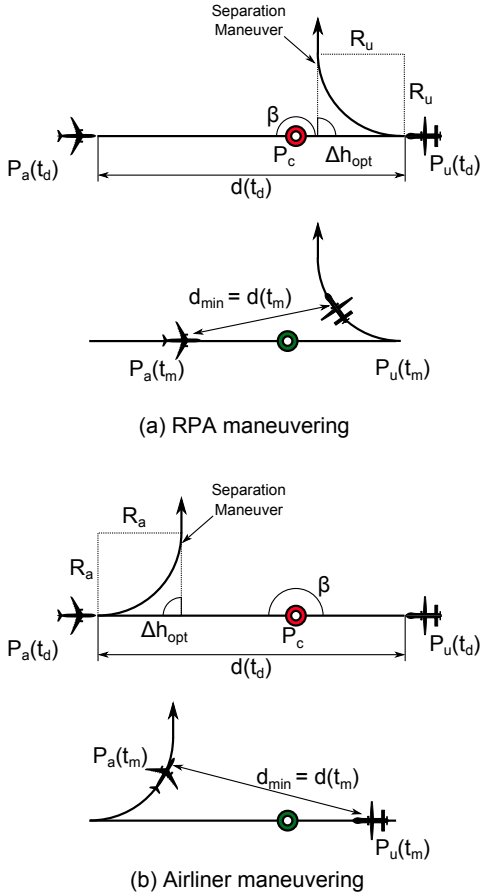

Fig. 2. Geometries for the separation manoeuvres.

point in the flight plan). We define t_d as the instant of time when the separation conflict is detected. ADS standards specify that intruders shall be detected at a constant minimum time, regardless of the conflict geometry [21]. Thus, typical radiation patterns for ADS antennae are not omnidirectional, as shown in Fig. 3.

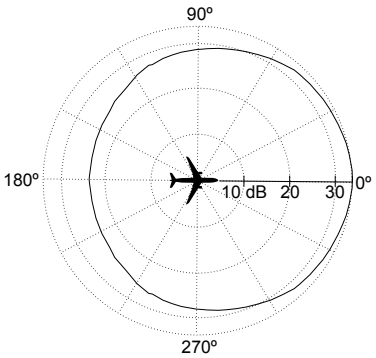

Fig. 3. Radiation pattern of an ADS antenna

According to the depicted conflict scenario, at t_d the airliner is located at point $P_a\,(t_d)$, while the RPA is at $P_u\,(t_d)$ and they are separated a distance $d\,(t_d)$. The conflict geometry is defined by the angle β that can range from $0°$ up to $360°$. Both aircraft are moving towards the same position (P_c) and will arrive there at the same time.

In order to avoid this separation conflict, one of them will change its trajectory, being Δh_{opt} the heading change with which the minimum distance between aircraft (d_{min}) is maximised. The computation of this optimal heading change was already presented in [18], [20]. Results showed that if we take into account the performance dissimilarities in terms of speed and bank angle, the minimum separation distance will be greater if the fastest aircraft performs the separation manoeuvre; that is, the airliner. Yet, it is worth assuming that in the future, manned commercial flights might have higher priority than the RPAS when facing conflicting trajectories. Thus, both cases will be analysed in this paper.

Moreover, if the minimum separation distance between aircraft is set to a fixed value, as typically occurs in controlled airspace, we can define the reaction time t_r as the time elapsed between the instant the conflict is detected (t_d) and the last time that the minimum separation distance could be maintained if the reaction manoeuvre is applied.

B. Optimal Separation Angles

We will use a forward conflict ($\beta = 180°$) to exemplify this scenario (see Figures 4 and 5. In Fig. 4 the conflicting aircraft are an Airbus A320 and a Boeing 737, having both similar cruise speeds, while in Fig. 5 the Airbus A320 trajectory is in conflict with an MQ-9 RPA. For both figures, the plot on the left shows the results when the slowest aircraft performs the heading change, while the plot on the right shows the case when the fastest aircraft manoeuvres. The x-axis represents Δh, while in the y-axis depicts the minimum distance between the aircraft. Each line of the plots represents a different Time to Conflict t_c, which is discretised in steps of 1 minute, from 2 to 10 minutes.

As expected, the lower the t_c, the lower minimum separation distance achieved for a given Δh. Moreover, when aircraft speeds are dissimilar, clear differences appear depending on who performs the separation manoeuvre. For example, as seen in Fig. 5, if the aircraft are situated at $t_c = 5$ minutes from the conflict point and the reaction manoeuvre is performed at $\Delta h = 20°$, the minimum achieved separation distance is either 14 NM or only 5 NM depending on who performs the manoeuvre. The reader is referred to [18] for more examples and a detailed analysis of the different geometries.

III. Enhanced analysis for the RPAS separation manoeuvres

The initial separation analysis performed so far does not take into account some effects that may have a negative impact in the execution of the separation manoeuvres: essentially the RPA bank angle limitations and dynamics. For RPAS operating at high altitudes these limitations are not negligible. Fig. 6 depicts a more detailed conflict scenario in which bank angle

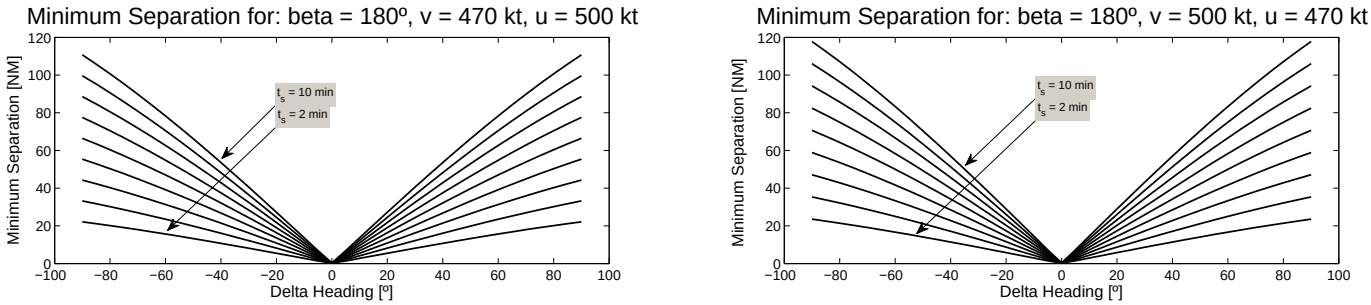

Fig. 4. Forward conflict in which (a) the slower B737 performs a separation heading change and (b) the fastest A320 performs the heading change.

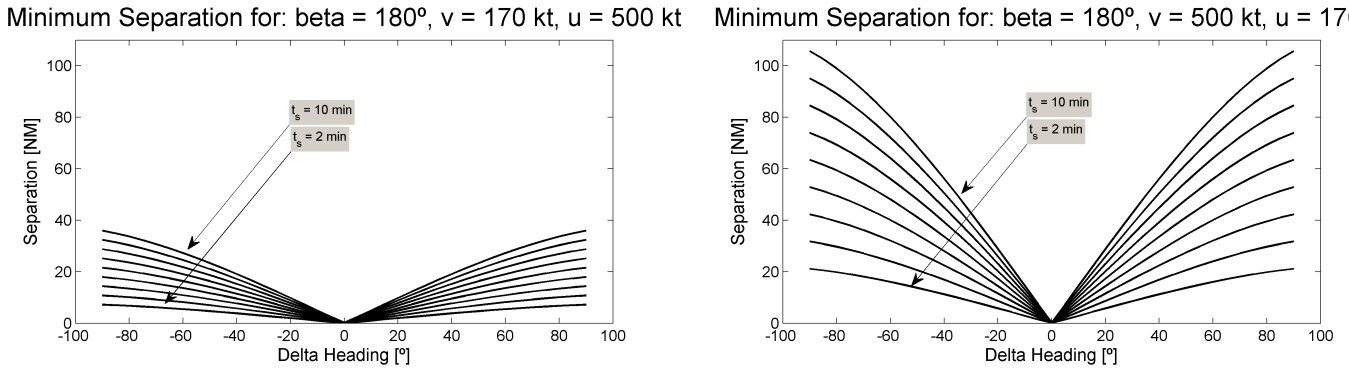

Fig. 5. Forward conflict in which (a) a MQ-9 performs a separation heading change and (b) an A320 performs the heading change.

and roll factors are taken into account for backward conflicts (lateral and oblique/forward conflicts need a similar analysis).

A. Analysis of backward separation manoeuvres

Let us assume an RPA that predicts a separation conflict with an airliner and determines the optimal heading change needed to maintain a certain separation distance (such for example 5NM). The resulting trajectory will be that strictly complying with this separation minima, i.e. all trajectories executed later (regardless the heading change) will result into a loss of separation.

The ability of the RPA to properly intercept the desired separation trajectory is determined by its turning performance and by the anticipation used to initiate the manoeuvre, thus compensating the actual turning limitations. Once the RPA pilot has committed to execute the separation manoeuvre, the RPA will initiate its heading change. However, when modelling the turn behaviour of the RPA it is well accepted to assume a certain delay in order to model the roll time (the time required to achieve the turning bank angle). This time mainly depends on the handling qualities of the aircraft, its speed and to a lesser extent the altitude. After this initial roll time, the RPA is assumed to start changing the heading (as a function of the bank angle and speed).

Multiple turning scenarios exist depending on the instant in which the RPA initiated its manoeuvre when reacting to a forward conflict. In Fig. 6, following the trajectory labeled A, the RPA initiates the manoeuvre with the exact timing producing a perfect turn that later on intercepts the separation trajectory at point A'. From then on, the RPA will roll back to follow a straight trajectory until the conflict is cleared. If the RPA performs as described, it will never violate the minimum separation distance.

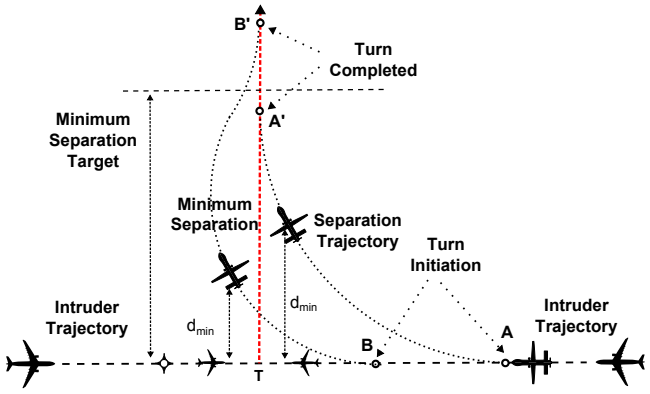

Fig. 6. Turn limitation effects for forward/backward separation conflicts.

On the contrary, if the RPA delays its turn until reaching point B (due to a late decision or due to a bad turning model), a loss of separation will occur. In this situation the RPA will turn right until a point in space in which it will roll back to the left in order to intercept the separation trajectory from the other side at point B'. During this period of time the RPA

has been flying beyond the theoretical separation trajectory, although the separation between the RPA and the intruder may not be breached if the intruder is distant enough.

The main question to respond is to determine if the instant in which both the RPA and the airliner reach their minimum separation distance occurs before or after the RPA has been able to intercept back the theoretical separation trajectory. Our analysis will limit the number of turning manoeuvres to those executed just after surpassing the optimal turning point A until the theoretical turning point T. We discuss in detail the scenario in which a RQ-4 Global Hawk performs a separation turn as the impact of the speed on the turn limitations is much important than for a MQ-9 Reaper (170 kt). In fact, results demonstrate that this effect is almost negligible for a MQ-9, but not for a RQ-4.

B. Turn limitations and delays as a function of the intruder speed

Figures 7, 8 and 9 depict the simulation results when calculating the minimum separation distance as a function of the intruder speed and the turn delay for the backward conflict geometry when the turn limitations of the RPA are taken into account. A Time to Conflict (t_c) of 5 minutes is applied in each figure. All of them plot, in the x-axis, the intruder speed (a range from 400 up to 600 kt has been considered) while, in the y-axis the minimum distance (in NM) is depicted. Each line represents a different delay, ranging from 0 up to 25 seconds.

The coloured little circles show when the minimum distance has been achieved: the green ones set it in the first stage (the RPA is turning while crossing the theoretical separation trajectory), the yellows in the second (the RPA rolls back to adjust to the theoretical trajectory)and, finally, the blues in the third (the RPA is already following that trajectory). Finally, the red line indicates the achieved separation distance when no turn limitations or delays are applied; this is, when applying an instantaneous 90 degree heading change. Figure 7 represents the case when the speed of the RPA is set to 170 kt. The time when the minimum separation distance is achieved occurs after the RPA turn manoeuvre is performed regardless the considered intruder speed and delays. Hence, we can conclude that the effect of turn limitations over the achieved separation distance can be modelled as an instantaneous turn and a constant offset.

When increasing the speed of the RPA the turn limitations should not be modelled as a constant, rather the detailed turning trajectory should be considered. This is because the minimum separation distance is not achieved after the turn manoeuvre is completed but during that turn itself. Hence, the trajectory of the RPA when performing the turn should be taken into account. This effect is depicted in Figures 8 and 9. Figure 8 represents the case when the speed of the RPA is set to 250 kt. Several aspects have changed with regard to Fig. 7. First, the coloured circles now indicate that the time when the minimum separation distance is achieved occurs when the turn manoeuvre is being performed. For the lower range of considered intruder speeds this occurs during the first turn (green circles). On the other hand, as the intruder speed increases, this time is postponed to the second one (blue ones). Finally, in this case the delay is not negligible for the lower range of intruder speeds. The greater the turn is delayed the smaller separation distance is achieved.

If the RPA speed is increased, the effects of a limited bank angle and delay are greater. Figure 9 shows the case when it is set to 300 kt. Now the delay effects have been extended to the whole range of considered intruder speeds, being more important at lower speeds. Note that, in some cases, it is better to consider the turn limitations rather than considering the *ideal* case. This is because an instantaneous 90 degree heading change is not the optimal manoeuvre for resolving backward conflict geometries.

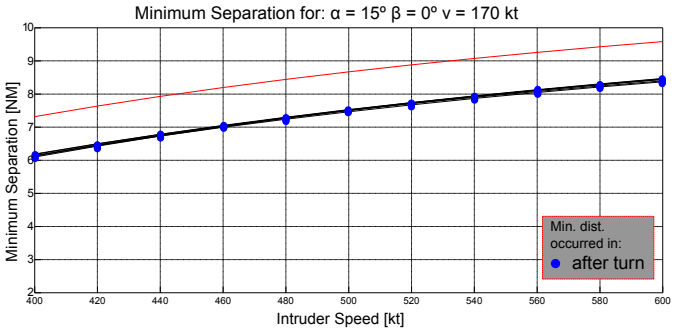

Fig. 7. Minimum separation for backward conflicts ($\beta = 0^o$) as a function of intruder speed where $\alpha = 15^o$ and $v = 170kt$.

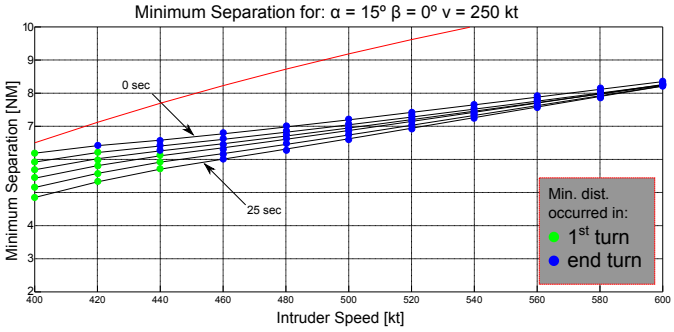

Fig. 8. Minimum separation for backward conflicts ($\beta = 0^o$) as a function of intruder speed where $\alpha = 15^o$ and $v = 250kt$.

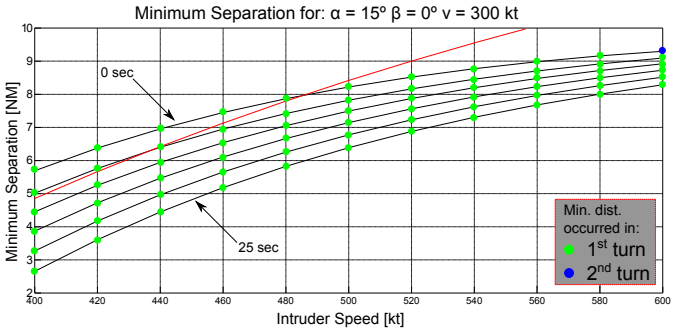

Fig. 9. Minimum separation for backward conflicts ($\beta = 0^o$) as a function of intruder speed where $\alpha = 15^o$ and $v = 300kt$.

C. Turn limitations and delays as a function of the bank angle

Figures 10, 11, and 12, show the simulation results for the backward conflict geometry. All figures plot, in the x-axis, the bank angle (from 5° up to 30°) and the minimum separation distance in the y-axis. Figure 10 depicts the result when the RPA speed is set to 170 kt. In this case, we can conclude that the minimum separation is not correlated with the delay, at least for bank angles greater than 7 degrees. Regarding the relation between the separation distance and the bank angle, it can be seen a local minimum of 6.5 NM when the bank angle is approximately 8 degrees. Nevertheless, the variation of the minimum distance with the bank angle is small.

Results presented in Fig. 10 are not valid when the RPA speed is increased. Figure 11 shows the results for the same simulations but, in this case, the RPA speed is set to 250 kt. The local minimum depicted in Figure 11 has been displaced to a greater value of bank angle. Unlike before, the delay time is correlated with the minimum distance for the lower range of bank angle values. Moreover, there is a local maximum in the lower range of bank angle, when it is set to 8 degrees. Hence, in these conditions it is better to perform the turn manoeuvre with a small bank angle, around 8 degrees, rather than executing it with a 30 degree. In addition, the minimum distance will be achieved even before finishing the first turn since a heading change of 90 degrees is not necessary to achieve the maximum separation.

If the RPA speed is increased (Fig. 12)the previously explained results are extended. The variation of the minimum distance regarding the delay is more pronounced. Both local minimum and maximum values are displaced to greater values of bank angle. For this particular case, the optimal value of bank angle in order to achieve the maximum separation distance is approximately 10 degrees. Summing up, when the speeds of both aircraft are more similar, the separation manoeuvre should be *softer* from the bank angle point of view.

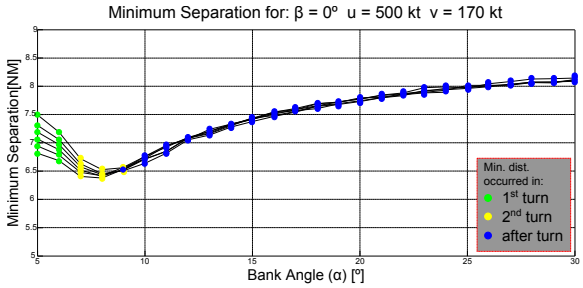

Fig. 10. Minimum separation for backward conflict as a function of RPA bank angle where $u = 500kt$ and $v = 170kt$.

IV. Feasibility of the Separation Manoeuvres

Separation conflicts involving an airliner and a RPA may be resolved by means of changing any of their own trajectories or flight level. Even though vertical manoeuvring may be possible and even desirable, altitude changes greatly affect RPAS performing surveillance operations and even RPAS may suffer from vertical speed limitations at high altitudes. Given

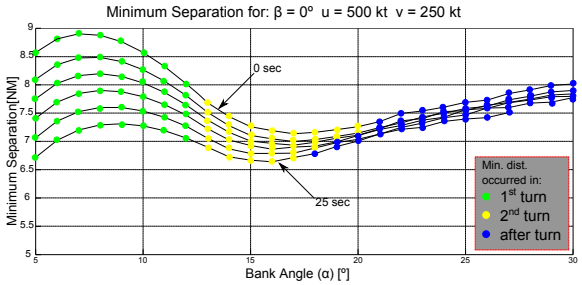

Fig. 11. Minimum separation for backward conflict as a function of RPA bank angle where $u = 500kt$ and $v = 250kt$.

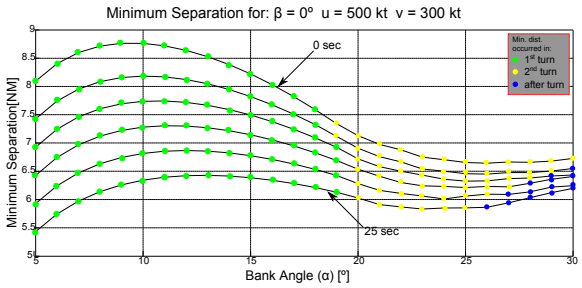

Fig. 12. Minimum separation for backward conflict as a function of RPA bank angle where $u = 500kt$ and $v = 300kt$.

these conditions, we will strictly focus on lateral separation manoeuvres, in which three different situations arise (all of them are depicted in Fig. 13).

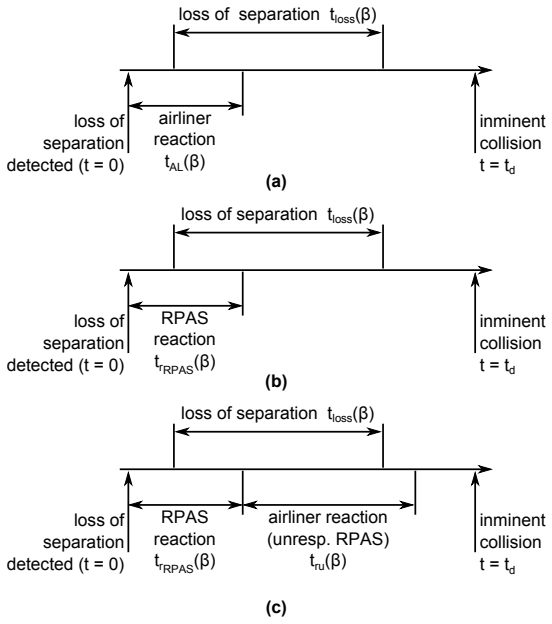

Fig. 13. Separation conflict resolution: (a) the airliner manoeuvres; (b) the RPAS manoeuvres; (c) an unresponsive RPAS.

If we assume that a potential loss of separation is detected at a certain instant of time $t = 0$, the possible collision will occur at $t = t_d$. In the event that the separation conflict has been detected by means of ADS-B, t_d will remain constant regardless the conflict geometry β (recall Fig. 3). Let be $t_{loss}\,(\beta)$ the instant of time when the required lateral separation

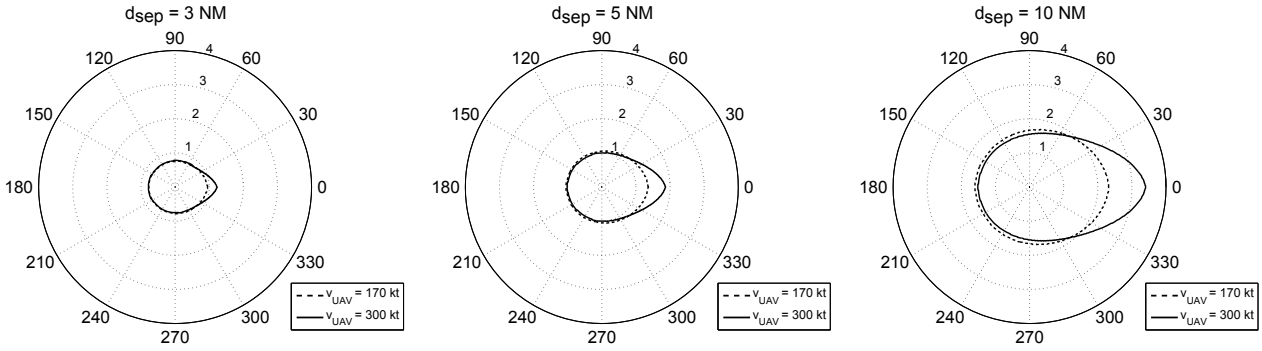

Fig. 14. Reaction polar charts when the airliner performs the separation manoeuvre (from left to right, $d_{sep} = \{3, 5, 10\}$ NM).

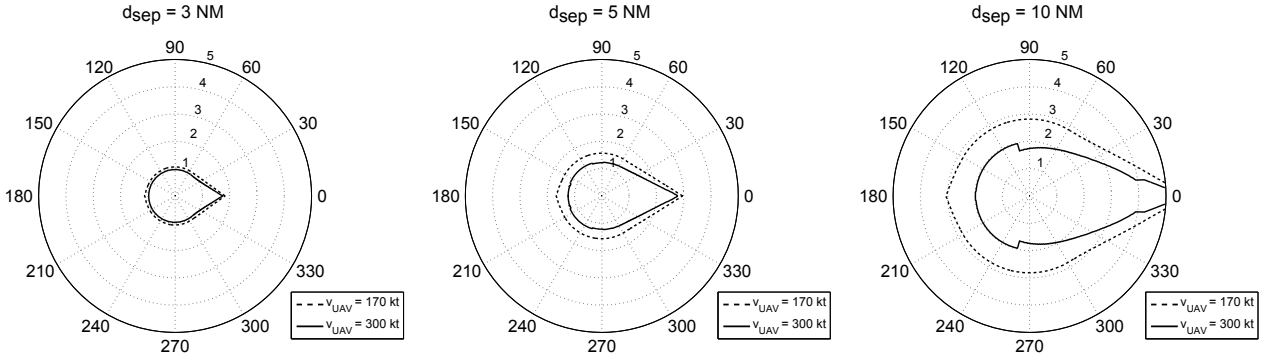

Fig. 15. RPA performs the separation manoeuvre for $d_{sep} = \{3, 5, 10\}$ [NM]. The whole range of β is plotted against the reaction time $t_{r_{RPA}}$.

is transgressed. t_{loss} clearly depends on β and therefore, it will vary as a function of the conflict geometry. On the other hand, let be $t_{AL}(\beta)$, $t_{RPAS}(\beta)$ the airliner and RPAS reaction times, respectively. They depend on the conflict geometries too. Finally, $t_{ru}(\beta)$ represents the remaining time that the airliner has to perform the separation manoeuvre in the case of an unresponsive RPAS.

Figure 13 (a) shows the case where the ATCo commands the airliner to perform the separation manoeuvre. The required separation will not be transgressed if $t_{AL} < t_{loss}$ for the β of the conflict geometry. On the other hand, Fig. 13 (b) depicts the case when the RPAS is commanded to perform the manoeuvre. The required separation will only be maintained if $t_{RPAS} < t_{loss}$ for the conditions of the conflict geometry. Finally, Fig. 13 (c) represents the most challenging case: if the ATC controller has commanded the RPAS to perform the manoeuvre, but the RPAS keeps unresponsive, how much remaining time does the airliner have to perform itself the separation manoeuvre before breaching the required lateral separation? In the worst case, $t_{ru} = t_d - t_{RPAS} - t_{loss}$. Hence, if $t_{ru} < t_{AL}$, the required separation could be maintained.

A. The airliner manoeuvres to maintain separation

Figure 14 shows the reaction polar charts when the airliner is the one that performs the separation manoeuvre. In the radial dimension the reaction time $t_{r_{AL}}$ has been plotted while, in the angular one, the conflict angle β has been depicted. The airliner speed is 500 kt for all the charts, but two different RPA speeds (v_{UAV}) of 170 and 300 kt have been considered and represented using dotted and patterned lines, respectively. Each plot depicts a specific minimum lateral separation, from left to right $d_{sep} = \{3, 5, 10\}$ NM.

All three charts are symmetrical about a horizontal axis crossing the coordinate origin. This is because the manoeuvring aircraft turns towards the direction in which the conflict will be better avoided. However, charts do not show any other type of symmetry. Hence, $t_{r_{AL}}$ will vary depending on β. Moreover, it can be seen that $t_{r_{AL}}$ increases if the minimum separation requirement does. Furthermore, t_r remains almost constant for a specific v_{uav}, except when $\beta \approx 0°$ (i.e. a backward conflict). Here, t_r increases significantly. For all considered cases, $t_{r_{AL}}$ remains below the instant of time when the minimum required lateral separation is transgressed t_{loss}. Hence, a potential separation conflict could be avoided if the airliner is the aircraft commanded to manoeuvre.

The chart on the left shows the situation when the minimum separation distance d_{sep} is set to 3 NM. In this case, t_r remains almost constant regardless β and below the one minute threshold, except when $\beta \approx 0°$ (backward conflict) and $v_{RPA} = 300$ kt. Here, $t_{r_{AL}}$ is increased up to 1.5 minutes. The chart on the middle plots the case when d_{sep} is set to 5 NM (the most usual lateral separation between aircraft in radar-controlled airspace).

Again $t_{r_{AL}}$ remains almost constant ($t_{r_{AL}} \approx 1$ min) for a wide range of β and for the two represented v_{RPA} values. Nevertheless, for the backward conflict, $t_{r_{AL}}$ is increased up to 1.75 min when $v_{RPA} = 300$ kt. Finally, the chart on the right, shows a conservative lateral separation ($d_{sep} = 10$ NM), confirms the trend of $t_{r_{AL}}$ to increase with respect to d_{sep}. In this case, when the RPA is flying at 300 kt, $t_{r_{AL}}$ for a backward conflict is increased up to 3.4 min.

B. The RPA manoeuvres to maintain separation

The lateral separation distance is better achieved if the airliner performs the separation manoeuvre. However, it might be the case that, due to the surrounding traffic or by assuming an hypothetical commercial aircraft priority, the RPA may be requested to perform the necessary separation manoeuvre.

Figure 15 depicts the reaction charts for the conflict geometry when the RPA performs the separation manoeuvre. Three charts are plotted, one per each required separation distance. Note that the evolution of $t_{r_{RPA}}$ throughout the three charts is the same as $t_{r_{RPA}}$; that is, it increases with d_{sep}. However, the increasing rate now is much higher, specially when $\beta \approx 0°$, almost regardless of v_{RPA}. For values of $\beta \not\approx 0°$, t_r ranges from 1 up to 3 minutes, depending on v_{RPA}. In case of a required lateral separation of 5 NM, $t_{r_{RPA}} \approx 1.5min$ when $\beta \not\approx 0°$; thus, the lateral separation can be properly maintained. Even in the case when $\beta \approx 0°$, $t_{r_{RPA}}$ does not exceed 3 minutes. However, the problem arises when the required separation is increased up to 10 NM. For most β values the separation can be well maintained. However, when facing a backward conflict the lateral separation minima is violated regardless the considered RPA speeds.

C. An unresponsive RPAS

Another factor that must be taken into account is the fact that when the RPA is commanded to manoeuvre, all the sudden it may become unresponsive. Then, the only way to resolve the separation conflict is to command the airliner to perform the manoeuvre. In this situation, the worst case occurs when the RPA tried to perform the heading change only t_r minutes prior to the occurrence of the potential collision.

Figure 16 depicts the resulting charts assuming the three different required lateral separations. The dark lines represent the remaining time after the RPA suddenly becomes unresponsive and before the potential collision may occur; this is, $t_d - t_{r_{\mathrm{RPA}}}$. On the other hand, in light gray, the airliner reaction times have been overlapped.

When d_{sep} is set to 3 NM, there are no intersections between the light gray lines and the black ones. Hence, the airliner has enough time to manoeuvre maintaining the required lateral separation regardless of the conflict geometry. In the worst case, when facing a backward conflict, the remaining time is greater than two minutes. If $d_{sep} = 5$ NM is required, there are no intersections as well. However, the remaining reaction time has been drastically reduced, specially in the backward conflict region. In that region, the light gray and black lines are extremely close to each other, hence, the remaining reaction time is close to 0, hence, a loss of separation may occur.

This situation is caused by two different factors. First, according to Fig. 15, for a required separation of 10 NM, when $\beta \approx 0°$ the lateral separation cannot be maintained if the RPA performs the heading change. Therefore, $t_d - t_{r_{RPA}}$ will be negative for these range of β values. Second, for some $\beta \not\approx 0$ values, $t_d - t_{r_{RPA}} > 0$ but $t_d - t_{r_{RPA}} - t_{r_{AL}}$ will be negative. In those cases, the loss of separation will also occur. Thus, according to Fig. 16 when $\beta \in \{-30°, 30°\}$, the separation manoeuvre should never be performed by the RPA.

V. The operational point of view

The results presented in Fig. 16 revealed the relationship between the required lateral separation distance, the RPA and airliner velocities (v_{UAV}, v_{AL}) and the conflict angle β. However, from an operational point of view, these results must be simplified to make them useful. This simplification leads to define similar separation conflict areas. Figure 17 brings out the general strategy and Tab. I summarises it.

The figure shows the same charts as in Fig. 16 but different areas have been highlighted as a function of the severity of a loss of separation scenario. The green areas represent the geometries where the airline has enough time to react, in case the RPAS is not manoeuvring. The red areas show the cases where a loss of separations will always occur, since the airliner does not have enough time to react once the RPAS has been detected unresponsive. Finally, a yellow zone is represented indicating that the reaction time for the airliner is rather *small*.

Required Separation Distance	**Low Risk β range**	**Medium Risk β range**	**High Risk β range**
3 NM	$[0°, 360°]$	N/A	N/A
5 NM	$[45°, 315°]$	$[10°, 45°]$ $[-45°, -10°]$	$[-10°, 10°]$
10 NM	$[90°, 270°]$	$[60°, 90°]$ $[-60°, -90°]$	$[-60°, 60°]$

TABLE I. β RANGES FOR THE OPERATIONAL RISK ZONES.

As seen in Fig. 17 for a minimum separation distance of $d_{sep} = 3$ NM the airliner has enough time to react regardless the conflict geometry (angle β). As d_{sep} increases, the remaining time that the airliner has to react in case of an unresponsive RPAS decreases. This is crucial for backward conflicts, which for $d_{sep} = 5$ NM the airliner has almost no time left to react. We arbitrarily set a yellow *warning zone* for $\beta \in [10°, 45°]$ and $\beta \in [-45°, -10°]$. In the event of an extended required lateral separation of d_{sep} = 10 NM the zone in red is obviously larger, with β values ranging from $-60°$ up to $60°$. In this case, the yellow zone has been rounded to β angles ranging form $[60°, 90°]$ and $\beta \in [-60°, -90°]$.

Concluding, different risk zones have been identified and simplified as a function of the results on the remaining reaction time studied in Section IV in order to make them meaningful from an operational point of view. These extension and location

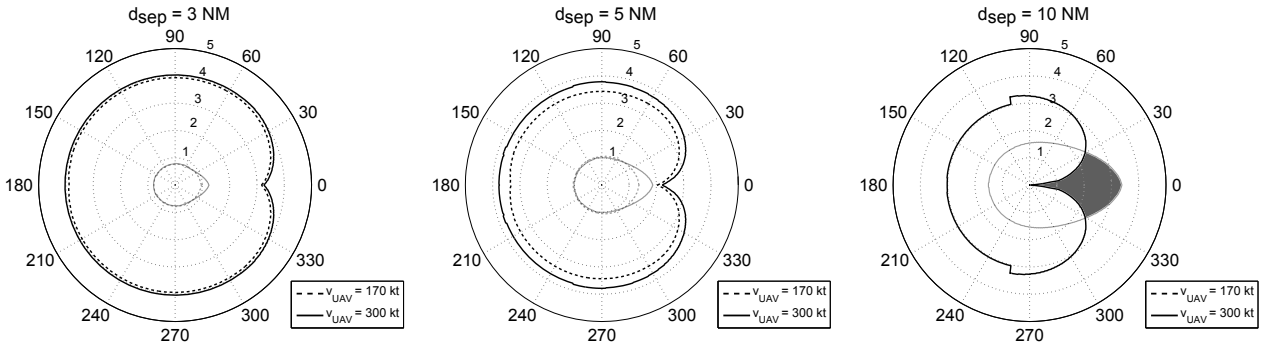

Fig. 16. Airliner performs the separation manoeuvre for an unresponsive RPA for $d_{sep} = \{3, 5, 10\}$ [NM]. The whole range of β is plotted against the reaction time t_{ru}.

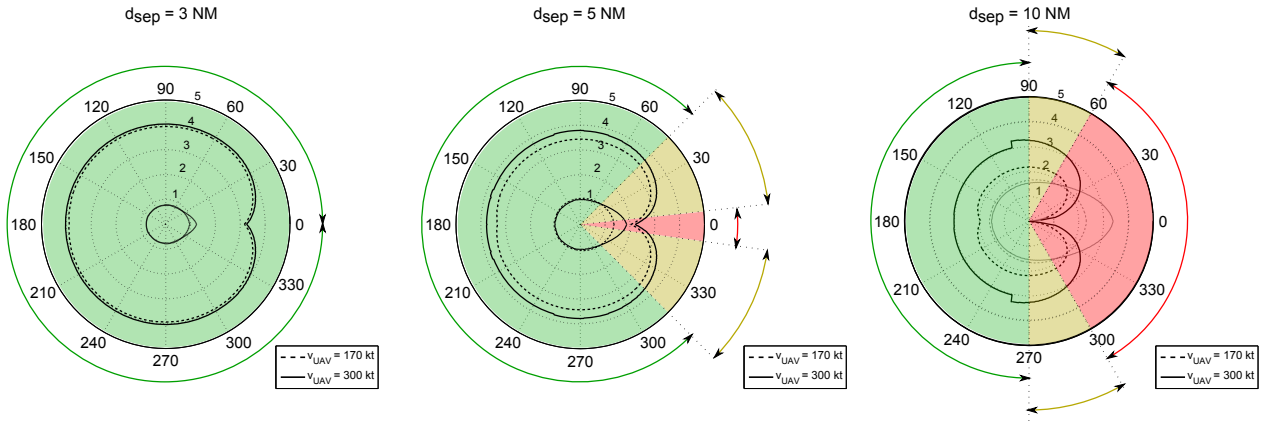

Fig. 17. Operational charts for the resolution of separation conflicts for $d_{sep} = \{3, 5, 10\}$ NM respectively. Green areas: airliner can react properly even in the case of an unresponsive RPAS; yellow: airliner can perform the manoeuvre but has to react quickly; red: a loss of separation situation would arise.

of these risk zones vary as a function on the required lateral separation distance, being more restrictive when increasing it.

VI. Conclusions and Future Work

A critical requirement for the integration of RPAS into non segregated airspace is to achieve safe separation between all surrounding traffic. This paper has analysed in depth the behaviour of the lateral separation when an airliner enters in conflict with a RPA, taking into account the peculiarities and the performance dissimilarities of both types of aircraft. The manoeuvring reaction times have been accurately calculated for the whole range of conflict geometries. Results show that backward separation conflicts (i.e. when both aircraft fly with the same heading) are the worst case scenario, specially when an unresponsive RPA is commanded to perform the heading change.

Based on this result, the paper has introduced a simplification of the reaction times and conflict geometries by grouping them regarding the probability of a loss of separation event. Three levels of likelihood have been proposed. The soundness of the concept will be validated by means of a real-time simulation environment that combines an ATC and RPAS detailed operation.

Acknowledgment

This work is funded by the European Organization for the Safety of Air Navigation (EUROCONTROL) under its CARE INO III programme. The content of the work does not necessarily reflect the official position of EUROCONTROL on the matter.

References

[1] K. Dalamagkidis, K. P. Valavanis, and L. A. Piegl, *On integrating unmanned aircraft systems into the national airspace system: issues, challenges, operational restrictions, certification and recommendations*, ser. International series on intelligent systems, control, and automation: science and engineering, S. G. Tzafestas, Ed. Springer-Verlag, 2009, vol. 26.

[2] P. Ostwald and W. Hershey, "Helping global hawk fly with the rest of us," in *ICNS Conference*, 2007.

[3] M. Gillian, G. J., and V. Cox, "Integration of unmanned aircraft systems into the national airspace system. concept of operations v2.0," American Society of Testing & Materials, Tech. Rep., Sep 2012.

[4] H. H. Hesselink and D. R. Schmitt, "Uas air traffic insertion starts now," National Aerospace Laboratory NLR, Tech. Rep., 2011.

[5] S. Graham, W. Chen, J. De Luca, M. Kay, J.and Deschenes, V. Weingarten, N.and Raska, and X. Lee, "Multiple intruder autonomous avoidance flight test," in *Proocedings of the AIAA Infotech@Aerospace Technical Conference*. St. Louis, Missouri (USA): AIAA, Mar 2011, paper No 2011-1420.

[6] D. Alejo, R. Conde, J. Cobano, and A. Ollero, "Multi-UAV collision avoidance with separation assurance under uncertainties," in *Proceedings of the IEEE International Conference on Mechatronics (ICM 2009)*. Malaga, Spain: IEEE, April 2009, pp. 1–6.

[7] G. Spence, D. Allerton, R. Baumeister, and R. Estowski, "Real-time simulation of a distributed conflict resolution algorithm," in *Proceedings of the 26th Congress of the International Council of the Aeronautical Sciences (ICAS)*, Anchorage, Alaska (USA), Sep 2008.

[8] G. Dowek and C. Muoz, "Conflict detection and resolution for 1,2,..,N aircraft," in *Proceedings of the 7th AIAA aviation technology, integration and operations conference*. AIAA, Sep 2007.

[9] C. Carbone, U. Ciniglio, F. Corraro, and S. Luongo, "A novel 3d geometric algorithm for aircraft autonomous collision avoidance," in *Proceedings of the 45th IEEE Conference on Decision and Control*. IEEE, Dec 2006, pp. 13 –15.

[10] S. J. Cho, D. S. Jang, , and M. J. Tahk, "Application of TCAS-II for unmanned aerial vehicles," in *Proceddings of JSASS-KSASS Joint Symposium on Aerospace Engineering*, Nagoya, Japan, Oct 2005.

[11] S. Han and H. Bang, "Proportional navigation-based optimal collision avoidance for uavs," in *Proceddings of the 2nd International Conference on Autonomous Robots and Agents*, Dec 2004.

[12] R. E. Weibel and J. R. John Hansman, "Safety considerations for operation of unmanned aerial vehicles in the national airspace system," MIT International Center for Air Transportation, Tech. Rep., Mar 2005.

[13] R. E. Weibel, M. W. M. Edwards, and C. S. Fernandes, "Establishing a risk-based separation standard for unmanned aircraft self separation," in *Proceedings of the ninth USA/Europe Air Traffic Management Research & Development Seminar*. Berlin, Germany: Eurocontrol / FAA, June 2011.

[14] X. Prats, L. Delgado, J. Ramrez, P. Royo, and E. Pastor, "Requirements, issues, and challenges for sense and avoid in unmanned aircraft systems," *Journal of Aircraft*, vol. 49, no. 3, pp. 677–687, May-Jun 2012.

[15] ICAO, *Procedures for Air Navigation Services. Air Traffic Management*, 14th ed., International Civil Aviation Organisation, Montreal (Canada), 2001, doc. 4444.

[16] Eurocontrol, "Review of asas applications studied in europe," CARE/ASAS Action. CARE/ASAS Activity 4, Technical report, Feb 2002, available at: http://www.eurocontrol.int/care-asas/gallery/content/public/docs/act4/care-asas-a4-02-037.pdf.

[17] G. Bartkiewicz, "Enhancement of airborne conflict prediction times through automatic dependent surveillance-broadcast (ADS-B) transmitted trajectory intent information," in *Proceedings of the 20th Conference on Digital Avionics Systems (DASC)*, vol. 2. AIAA, oct 2001, pp. 7B1/1 –7B1/11.

[18] M. Prez-Batlle, E. Pastor, and X. Prats, "Evaluation of separation strategies for unmanned aerial systems," in *Proceedings of the 5th International Congress on Research in Air Transportation (ICRAT)*. Berkeley, California (USA): EUROCONTROL / FAA, May 2012.

[19] M. Prez-Batlle, E. Pastor, P. Royo, X. Prats, and C. Barrado, "A taxonomy of uas separation maneuvers and their automated execution," in *ATACCS '12: Proceedings of the 2nd International Conference on Application and Theory of Automation in Command and Control Systems,*, E. Garcia, C. Johnson, W. V. Ochieng, P. Palanque, F. J. Saez, M. A. Vilaplana, and M. Winckler, Eds., HALA! SESAR network. Toulouse, France, France: IRIT Press, May 2012, pp. 1–11. [Online]. Available: http://dl.acm.org/citation.cfm?id=2325676&coll=DL&dl=GUIDE&CFID=291851014&CFTOKEN=80853617

[20] E. Pastor, M. Prez-Batlle, P. Royo, R. Cuadrado, C. Barrado, and X. Prats, "On the design of uas horizontal separation maneuvers," in *Proceedings of the 2nd SESAR innovation days*. Braunschweig (Germany): SESAR, Nov 2012. [Online]. Available: http://www.sesarinnovationdays.eu/2012/papers

[21] I. A. AERONAUTICAL RADIO, "Arinc specification 424-15," Tech. Rep., February 2000.

AUTHOR BIOGRAPHY

Marc Perez-Batlle is an Aeronautical Engineer from the Technical University of Catalonia (Universitat Politècnica de Catalunya, UPC). He earned this degree on 2008. He also holds a degree in Telecommunications Engineering from the UPC. He earned this degree on 2012. He has been working with UPC since 2008 and, currently, he is an assistant professor at the School of Telecommunications and Aerospace Engineering of Castelldefels (EETAC).

Enric Pastor is a Computer Science Engineer from the Technical University of Catalonia (Universitat Politècnica de Catalunya, UPC). He received his Ph.D in Computer Architecture from the same university. He has been working with UPC since 1992 and currently, he is an associate professor at the School of Telecommunications and Aerospace Engineering of Castelldefels (EETAC).

Xavier Prats is an Aeronautical Engineer from the National School for Civil Aviation. He holds a degree in Telecommunications Engineering from the Technical University of Catalonia (Universitat Politècnica de Catalunya, UPC). He earned both degrees in 2001. He received his Ph.D in Aerospace Science and Technology from UPC in 2010. He is currently an assistant professor at the School of Telecommunications and Aerospace Engineering of Castelldefels (EETAC).

Pablo Royo is a Telecommunications Engineer from the Technical University of Catalonia (Universitat Politècnica de Catalunya, UPC). He also holds a Ph.D. in Computer Architecture from the same university. He has been working with UPC since 2009 and currently, he is a lecturer at the School of Telecommunications and Aerospace Engineering of Castelldefels (EETAC).

Raul Cuadrado is a Telecommunications Engineer from the Technical University of Catalonia (Universitat Politècnica de Catalunya, UPC). He has been working with UPC since 2006 and currently, he is an assistant professor at the School of Telecommunications and Aerospace Engineering of Castelldefels (EETAC).